

Tunneling between edge states in a quantum spin Hall system

Anders Ström and Henrik Johannesson

Department of Physics, University of Gothenburg, SE 412 96 Gothenburg, Sweden

We analyze a quantum spin Hall (QSH) device with a point contact connecting two of its edges. The contact supports a net spin tunneling current that can be probed experimentally via a two-terminal resistance measurement. We find that the low-bias tunneling current and the differential conductance exhibit scaling with voltage and temperature that depend nonlinearly on the strength of the electron-electron interaction.

PACS numbers: 73.43.-f, 73.63.Hs, 85.75.-d

A rapidly growing branch of condensed matter physics draws on the exploration of topologically nontrivial quantum states. Experimentally realized examples, which are by now well-understood, are given by the integer [1] and fractional [2] quantum Hall states. These states defy a classification in terms of the standard Ginzburg-Landau theory of symmetry breaking and a local order parameter, but can instead be characterized by a topological quantity [1, 2]. The importance of being able to identify a phase of quantum matter that does not fall under the Ginzburg-Landau paradigm has set off a search for other topologically nontrivial states, analogous to, but distinct from those connected to the quantum Hall effects.

Some time ago, Kane and Mele – building on work by Haldane [3] – discussed the possibility of a new type of “topologically ordered” state of electrons in two dimensions: a *quantum spin Hall (QSH) insulator*, proposed to be realized at low energies in a plane of graphene due to spin-orbit interactions [4]. Being a band insulator, a QSH insulator has a charge excitation gap in the bulk, but at its boundary there are gapless edge states with energies inside the bulk gap. These states, which come in an odd number of Kramers’ doublets, are “helical” (with clockwise/counterclockwise circling states carrying spin up/down, or vice versa, depending on the orientation of the effective electric field that enters the spin-orbit interaction) and are responsible for the intrinsic spin Hall effect that Murakami *et al.* had earlier predicted may occur in bulk insulators [5]. Time-reversal invariance implies that the energy levels of the counter-propagating edge states cross at particular points in the Brillouin zone. It follows that the spectrum of a QSH insulator cannot be continuously deformed into that of an ordinary band insulator, which has zero (or equivalently, an even number of) Kramers’ doublets. In this exact sense, a QSH insulator realizes a topologically nontrivial state of matter [6]. In subsequent and independent work, the QSH insulator state was proposed to occur also in strained semiconductors [7] and in HgTe quantum wells with an “inverted” electronic gap [8]. An experiment carried out on quasi-two-dimensional HgTe quantum wells grown by molecular beam epitaxy and sandwiched between (Hg,Cd)Te barriers has revealed data consistent with helical edge state transport, suggesting the first observation of the

QSH effect [9]. The possibility of dissipationless transport of spin currents along the edges of a QSH insulator is a tantalizing prospect for future spintronics applications [10]. To make progress, however, a more complete picture of the physics is required.

An important issue is to understand the behavior of edge currents in the presence of a tunneling junction connecting two opposite edges of a QSH bar (FIG. 1). When the bar is connected to a battery, a net spin current can tunnel through the junction, and one would like to know how the electron-electron interaction influences its conductance. This is the problem we shall address here.

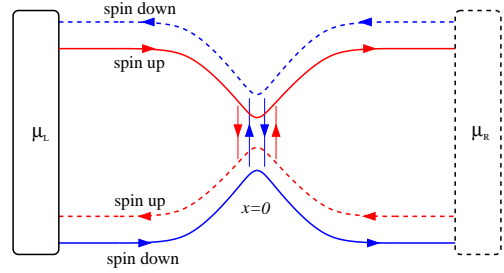


FIG. 1: (Color online) Geometry of the QSH point contact device studied in this paper. The full (dotted) lines represent helical edge states in equilibrium with the left (right) contact.

We consider the simplest situation with a single Kramers’ doublet of helical edge states, applicable to a tunneling experiment on a HgTe quantum well [9]. In the absence of electron interactions this case can formally be thought of as resulting from a superposition of two integer quantum Hall systems with the up- and down-spins of the electrons being subject to opposite effective magnetic fields. This emulates the spin-orbit interaction that is built-in in the k - p Hamiltonian that defines the electron dynamics close to the Fermi level of the quantum well [9]. The bar is connected to a battery with left (L) and right (R) contacts as in FIG. 1. Applying a gate voltage V_g perpendicular to the upper and lower edge of the bar at $x = 0$ will bring the edges close to each other, forming a point contact at which electrons may tunnel from one edge to the other. With the gate voltage turned off there is no tunneling present, assuming the edges to be well separated. For the case illustrated

in FIG. 1, electrons originating in the L [R] contact of the battery carry current to the right [left], with spin-up [spin-down] on the upper edge and spin-down [spin-up] on the lower edge. The right- [left-] moving electrons are in equilibrium with the left [right] contact and have a Fermi energy equal to the electrochemical potential μ_L [μ_R] of that contact. Note that counterpropagating electrons do not equilibrate when injected at different chemical potentials since any scattering off impurities or defects conserves spin, thus making impossible transfer of electrons from one type of edge state to the other. If the driving voltage $V \equiv (\mu_L - \mu_R)/e > 0$, a net charge current flows from left to right on each edge, accompanied by a spin current carrying spin-up [spin-down] on the upper [lower] edge. Neglecting electron interactions, the ratio of the drain-source charge [spin] edge current to the driving voltage is the Hall [spin Hall] conductance e^2/h [$e/4\pi$] [11]. When the gate voltage V_g is turned on, more of the right-moving electrons tunnel through the point contact at a finite driving voltage $V > 0$, leading to a depletion of the source-drain current. While there is no net tunneling of charge between the edges, the point contact supports a net inter-edge spin tunneling current (cf. FIG. 1).

The picture becomes more complex when allowing for electron-electron interactions at the edges. Away from half-filling of the one-dimensional (1D) band of edge states, time-reversal invariance constrains the possible scattering processes at an edge to dispersive (d) and forward (f) scattering [12, 13]. In the vicinity of the Fermi points the corresponding interactions are given by

$$H_d = g_d \int dx \left(\psi_{R\uparrow}^\dagger \psi_{R\uparrow} \psi_{L\downarrow}^\dagger \psi_{L\downarrow} + \psi_{L\uparrow}^\dagger \psi_{L\uparrow} \psi_{R\downarrow}^\dagger \psi_{R\downarrow} \right) \quad (1)$$

and

$$H_f = g_f \sum_{\substack{\alpha=R,L \\ \sigma=\uparrow,\downarrow}} \int dx \psi_{\alpha\sigma}^\dagger \psi_{\alpha\sigma} \psi_{\alpha\sigma}^\dagger \psi_{\alpha\sigma}. \quad (2)$$

Here $\psi_{R\uparrow}$ and $\psi_{L\uparrow}$ are 1D fields that annihilate an electron in a clockwise propagating helical state on the upper and lower edge, respectively. Similarly, $\psi_{L\downarrow}$ and $\psi_{R\downarrow}$ are fields that correspond to a counterclockwise propagating state on the upper and lower edge, respectively. It is here important to emphasize that the presence of the dispersive scattering channel, controlled by (1), is a fundamental difference between the edge physics of a QSH insulator and a system exhibiting the integer quantum Hall effect (IQHE). As a result, the QSH insulator may show interaction effects which are suppressed in the IQHE. Adding a linearized kinetic term

$$H_0 = -iv_F \sum_{\sigma=\uparrow,\downarrow} \int dx \left(\psi_{R\sigma}^\dagger \partial_x \psi_{R\sigma} - \psi_{L\sigma}^\dagger \partial_x \psi_{L\sigma} \right), \quad (3)$$

we can bosonize $H = H_0 + H_d + H_f$, and obtain

$$H = \frac{v}{2} \sum_{i=1,2} \int dx \left(\frac{1}{K} (\partial_x \phi_i)^2 + K (\partial_x \theta_i)^2 \right), \quad (4)$$

with $K = \sqrt{\frac{2\pi v_F + g_f - 2g_d}{2\pi v_F + g_f + 2g_d}}$, and $v = \sqrt{(v_F + \frac{g_f}{2\pi})^2 - (\frac{g_d}{\pi})^2}$, v_F being the Fermi velocity. The indices 1 and 2 label the upper and lower edge, respectively, with $\phi_1 = \phi_{R\uparrow} + \phi_{L\downarrow}$, $\phi_2 = \phi_{L\uparrow} + \phi_{R\downarrow}$, $\theta_1 = \phi_{R\uparrow} - \phi_{L\downarrow}$, and $\theta_2 = \phi_{L\uparrow} - \phi_{R\downarrow}$, where $\phi_{\alpha\sigma}$ and $\theta_{\alpha\sigma}$ define chiral boson fields and their duals within the standard bosonization scheme [14]. Note that in contrast to an ordinary spinful Luttinger liquid which exhibits spin-charge separation, the boson fields in (4) contain both charge and spin. While helicity makes spin a redundant quantum number on a single edge, it is important to include it when two edges are connected via a point contact. The tunneling through the contact, with amplitude u , is governed by the operator

$$H_t = u \left(\psi_{L\uparrow}^\dagger \psi_{R\uparrow} + \psi_{R\uparrow}^\dagger \psi_{L\uparrow} + \psi_{R\downarrow}^\dagger \psi_{L\downarrow} + \psi_{L\downarrow}^\dagger \psi_{R\downarrow} \right), \quad (5)$$

defined at $x = 0$. It can similarly be bosonized:

$$H_t = \frac{2u}{\pi} \sin[\sqrt{\pi}(\phi_1 + \phi_2)] \cos[\sqrt{\pi}(\theta_1 + \theta_2)]. \quad (6)$$

Given the bosonized theory, eqs. (4) and (6), we may now use standard perturbative RG arguments to uncover the effect of electron interactions on the tunneling.

As a first step, we integrate out the bosonic fields in the partition function of the system except at $x = 0$, thus obtaining a theory defined only at the location of the point contact [15]. With Λ an energy cutoff, and $\tau = it$ Euclidean time, this gives

$$Z \sim \int \prod_{i=1,2} \mathcal{D}\phi_i \mathcal{D}\theta_i \exp(-S - S_t), \quad (7)$$

where

$$S = \sum_{i=1,2} \int_{-\Lambda}^{\Lambda} \frac{d\omega}{2\pi} |\omega| \left(\frac{1}{2K} |\phi_i(\omega)|^2 + \frac{K}{2} |\theta_i(\omega)|^2 \right) \quad (8)$$

and

$$S_t = -\frac{2u}{\pi} \int d\tau \sin[\sqrt{\pi}(\phi_1(\tau) + \phi_2(\tau))] \times \cos[\sqrt{\pi}(\theta_1(\tau) + \theta_2(\tau))]. \quad (9)$$

Next, the localized fields are split into slow (s) and fast (f) modes, $\phi_{is}(\tau) \equiv \int_{-\Lambda/b}^{\Lambda/b} \frac{d\omega}{2\pi} e^{-i\omega\tau} \phi(\omega)$ and $\phi_{if}(\tau) \equiv \int_{\Lambda/b < |\omega| < \Lambda} \frac{d\omega}{2\pi} e^{-i\omega\tau} \phi(\omega)$, with $b > 1$ a scale factor, and with a similar definition of θ_{is} and θ_{if} ($i = 1, 2$). A cumulant expansion in u then gives an expression for the low-energy effective action, call it S_{eff} . To $\mathcal{O}(u^2)$,

$$e^{-S_{eff}[\phi_s]} = e^{-S_s[\phi_s]} e^{\langle S_t \rangle_f - \frac{1}{2} \langle S_t^2 \rangle_f - \langle S_t \rangle_f^2 + \dots} \quad (10)$$

Here $S_s[\phi_s]$ is the slowly fluctuating part of S , while $\langle \dots \rangle_f$ is an average taken over the fast modes. The calculation of $\langle S_t \rangle_f$ and the second-order cumulant $\langle S_t^2 \rangle_f -$

$\langle S_t \rangle_f^2$ is here somewhat cumbersome, but is facilitated by the presence of the time-reversal symmetry. We find that

$$\langle S_t \rangle_f = \frac{2u}{\pi} b^{-\frac{1}{2}(K+1/K)} S_t[\phi_{1s}, \phi_{2s}, \theta_{1s}, \theta_{2s}], \quad (11)$$

with $S_t[\phi_{1s}, \phi_{2s}, \theta_{1s}, \theta_{2s}]$ as in (9) but with the slow fields replacing the original ones. As for the second-order term,

$$\langle S_t^2 \rangle_f - \langle S_t \rangle_f^2 = \frac{u^2}{\pi} \int d\tau (V_\theta \cos[\sqrt{\pi}(2\theta_1 + 2\theta_2)] + V_\phi \cos[\sqrt{\pi}(2\phi_1 + 2\phi_2)] + \dots), \quad (12)$$

where $V_\theta = b^{1-2/K} - b^{1-K-1/K}$, $V_\phi = b^{1-K-1/K} - b^{1-2K}$, and where ... indicate higher-order terms that do not influence the renormalization to this order in u . The first-order RG equation for u ,

$$\frac{du}{d \ln b} = u \left(1 - \frac{1}{2} \left(K + \frac{1}{K} \right) \right), \quad (13)$$

is obtained from (10) and (11) and reveals that the scaling dimension Δ_K of the tunneling operator H_t in (6) is $\Delta_K = \frac{1}{2}(K + 1/K)$. As for the second-order equations, these are extracted from (10) and (12), and read

$$\frac{dV_\theta}{d \ln b} = \frac{u^2}{\pi^2} \left(\left(1 - \frac{2}{K} \right) e^{(1-2/K) \ln b} - (1 - 2\Delta_K) e^{(1-2\Delta_K) \ln b} \right),$$

$$\frac{dV_\phi}{d \ln b} = \frac{u^2}{\pi^2} \left((1 - 2\Delta_K) e^{(1-2\Delta_K) \ln b} - (1 - 2K) e^{(1-2K) \ln b} \right).$$

These equations imply that, to second order in u , H_t renormalizes to zero for all values of K in the interval $1/2 < K < 2$. This includes the experimentally relevant regime for a HgTe quantum well: A rough estimate of K for this case, based on the approximate relation $K \approx (1 + U/(2E_F))^{-1/2}$ [16], yields that $0.8 < K < 0.9$, using that $E_F \approx \hbar/m^* r_s^2$ and $U \approx e^2/\epsilon r_s$, where e is the electron charge, $\epsilon \approx 20\epsilon_0$ is the dielectric constant, $m^* \approx 0.02m_e$ (with m_e the electron mass) [17], and where r_s is the effective Bohr radius for electron densities n_e in the interval $0.5 \times 10^{11} \text{ cm}^{-2} < n_e < 3.5 \times 10^{11} \text{ cm}^{-2}$ (at which the experiment in Ref. 9 was carried out).

It is interesting to compare the "weak-tunneling" fixed point found here to the situation for the quantum Hall effects, where for the IQHE the tunneling between edge states is marginal, while for the fractional quantum Hall effect the tunneling renormalizes to large values for all filling fractions [18]. In contrast, as seen from the second order RG equations above, a "strong-tunneling" QSH fixed point appears only for $K < 1/2$ (or for the unphysical region $K > 2$ with attractive electron interaction).

Turning to the tunneling current in the presence of a driving voltage $V = (\mu_L - \mu_R)/e$, we shall focus on the case of a low bias, allowing us to use a linear response formalism [19]. The current $I_c(t)$ that we shall calculate is the sum of the charge tunneling currents between edge states with the same helicity, related to the total spin

tunneling current $I_s(t)$ by $I_c(t) = (2e/\hbar)I_s(t)$. Since $I_c(t)$ is equal to the depletion of the charged source-to-drain current in the presence of the point contact (cf. FIG. 1), it follows that the spin current $I_s(t)$ can be detected experimentally by a two-terminal resistance measurement.

With $V > 0$, the current $I_c(t)$ can be expressed as the rate of change of the number of electrons in equilibrium with the left contact of the battery (see FIG. 1), $I_c(t) = -e\langle \dot{N}_L(t) \rangle$. The number operator $N_L = a(\psi_{R\downarrow}^\dagger \psi_{R\downarrow} + \psi_{R\uparrow}^\dagger \psi_{R\uparrow})$, where a is a lattice constant, has the property that $\dot{N}_L = i[H + H_t, N_L] = i[H_t, N_L]$. This implies that

$$I_c(t) = eu^2 \int dt' \Theta(t-t') \left(e^{ie \int_t^{t'} dt'' V(t'')} \langle [A(t), A^\dagger(t')] \rangle - e^{-ie \int_t^{t'} dt'' V(t'')} \langle [A^\dagger(t), A(t')] \rangle \right), \quad (14)$$

where $A = a(\psi_{L\uparrow}^\dagger \psi_{R\uparrow} + \psi_{L\downarrow}^\dagger \psi_{R\downarrow})$. Introducing the retarded Green's function $G_{ret}(t) = -i\Theta(t) \langle [A(t), A^\dagger(0)] \rangle$ and its transform $G_{ret}(-eV) = \int dt e^{-ieVt} G_{ret}(t)$, it follows that for constant V the integral in eq. (14) can be written as $-2\text{Im}[G_{ret}(-eV)]$. The correlation functions $G_+(t) = \langle A(t)A^\dagger(0) \rangle$ and $G_-(t) = \langle A^\dagger(0)A(t) \rangle$ are easily calculated in the bosonized theory, and one finds that

$$G_\pm(t) = \frac{1}{\pi} \left(\frac{a}{-v(t \pm i\delta)} \right)^{2\Delta_K}, \quad (15)$$

where δ is a short-time cutoff. Collecting the results,

$$I_c = 2eu^2 \frac{(a/v)^{2\Delta_K}}{\Gamma(2\Delta_K)} (eV)^{2\Delta_K-1}, \quad (16)$$

which tells us how the dc tunneling current scales with V in the limit $V \rightarrow 0$, and also how its amplitude depends on the parameter K that encodes the electron interaction. To account for the full K -dependence in eq. (16) one uses the parameterizations of K and v after eq. (4), with $ga \approx 4g_f$ [14]. To $\mathcal{O}(g_f/v_F)$, $v \approx v_F(5 + 3K)/(3 + 5K)$.

In order to extract the finite-temperature tunneling conductance G , we perform a conformal transformation of the correlation functions in (15), first going to Euclidean time $\tau = it$, and then taking $v\tau \rightarrow (v\beta/2\pi) \arctan(2\pi\tau/\beta v)$, with $\beta = 1/T$. It follows that

$$I_c = -2eu^2 (a/v)^{2\Delta_K} (2\pi T)^{2\Delta_K-1} \times \text{Im} \left[B(\Delta_K + ieV/2\pi T, \Delta_K - ieV/2\pi T) \times \frac{\sin(\pi(\Delta_K - ieV/2\pi T))}{\cos(\pi\Delta_K)} \right], \quad (17)$$

where B is the Euler beta function. In FIG. 2, the current is plotted for a few different values of K and T . We have here taken $a \approx 1 \text{ nm}$ and $v_F \approx 6 \times 10^6 \text{ m/s}$ [9, 17], and put $u = 0.1v_F/a$. From (17) we obtain the scaling of the zero-bias conductance G with temperature T ,

$$G \equiv \frac{dI_c}{dV} \Big|_{V=0} \propto T^{2\Delta_K-2}. \quad (18)$$

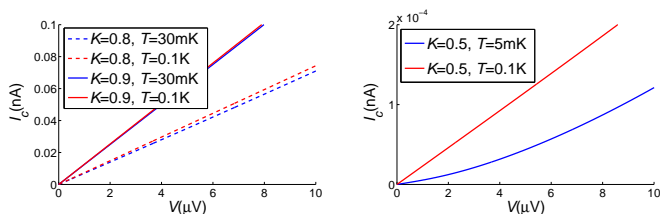


FIG. 2: (Color online) The two graphs show the charge tunneling current I_c as a function of the applied voltage V for different values of K and T . (The spin tunneling current I_s that transfers spin between the edges is given by $I_s = (\hbar/2e)I_c$.)

It is also interesting to explore the tunneling current for an ac voltage of the form $V(t) = V_0 + V_1 \sin(\Omega t)$. Inserting $V(t)$ into eq. (14) and following Ref. 20, we find that the dc component $I_{c,0}$ of the current, defined as the time average of $I_c(t)$, can be expressed as $I_{c,0} = 2eu^2(a/v)^{2\Delta_K} \sum_n a_n (eV_1/\Omega)(eV_0 + n\Omega)^{2\Delta_K-1}$, where $a_n(eV_1/\Omega) = \frac{1}{(2\pi)^2} \int_0^{2\pi} \int_0^{2\pi} dt dt' e^{in(t'-t)} e^{i\frac{eV_1}{\Omega}(\cos t' - \cos t)}$. In FIG. 3 we have plotted the dependence of $I_{c,0}$ on V_0 for some different values of K and V_1 . As seen from the figures, $I_{c,0}$ decreases with increasing electron-electron interaction (i.e. with decreasing values of K).

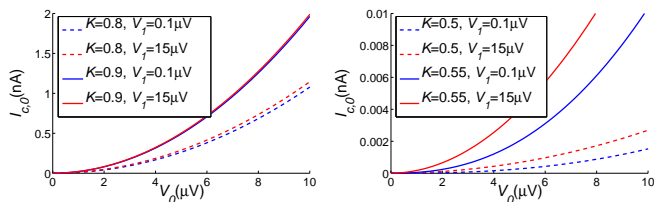


FIG. 3: (Color online) The dc component of the charge tunneling current $I_{c,0}$ as a function of V_0 for different values of K and V_1 . (The dc component of the accompanying spin tunneling current $I_{s,0}$ is given by $I_{s,0} = (\hbar/2e)I_{c,0}$.)

To summarize, we have found that a point contact connecting two edges of a QSH bar supports a spin tunneling current $I \propto V^{2\Delta_K-1}$ at small voltages V , with a zero-bias conductance $G \propto T^{2\Delta_K-2}$ for all values of $\Delta_K = (K + 1/K)/2$ with $1/2 < K < 2$, where K encodes the strength of the electron interaction. This spin current can be probed experimentally via a two-terminal resistance measurement. The interval $1/2 < K < 2$ contains the K -values applicable to a HgTe quantum well in the QSH regime [9]. When $K < 1/2$, the tunneling amplitude scales to large values, effectively severing the edges, analogous to what happens in a fractional quantum Hall system. Given that a QSH device can be manufactured which allows K to pass through the value of $1/2$, this would open for the possibility to experimentally study

the transition between strong and weak tunneling in a topologically nontrivial phase of matter.

We thank A. Brataas, S. Datta and A. Furusaki for valuable correspondence. This work was supported by the Swedish Research Council under grant 2005-3942.

Note added: Upon completion of this work we found a preprint by Hou *et al.* (arXiv:0808.1723v1, published in Ref. 21), on QSH edge states in a four-terminal corner junction geometry. For weak and intermediate electron interactions these authors find a weak-tunneling fixed point, similar to our result for a two-terminal device.

-
- [1] D. J. Thouless *et al.*, Phys. Rev. Lett. **49**, 405 (1982).
 - [2] X.-G. Wen and Q. Niu, Phys. Rev. B **41**, 9377 (1990).
 - [3] F. D. M. Haldane, Phys. Rev. Lett. **61**, 2015 (1988).
 - [4] C. L. Kane and E. J. Mele, Phys. Rev. Lett. **95**, 226801 (2005).
 - [5] S. Murakami, N. Nagaosa, and S.-C. Zhang, Phys. Rev. Lett. **93**, 156804 (2004).
 - [6] C. L. Kane and E. J. Mele, Phys. Rev. Lett. **95**, 146802 (2005).
 - [7] B. A. Bernevig and S.-C. Zhang, Phys. Rev. Lett. **96**, 106802 (2006).
 - [8] B. A. Bernevig, T. L. Hughes, and S.-C. Zhang, Science **314**, 1757 (2006).
 - [9] M. König *et al.*, Science **318**, 766 (2007).
 - [10] B. A. Bernevig and S. Zhang, IBM J. Res. Develop. **50**, 141 (2006).
 - [11] Note that the concept of a "spin Hall conductance" is well defined only when there is a fixed spin axis along which the edge modes are polarized. In a more realistic model, this may not be the case. As an example, an added Rashba-type spin-orbit interaction would produce an effective precession of the spin axis (while preserving time-reversal invariance). However, the measurable *charge properties* calculated in the present model are insensitive to whether the spin axis is pinned or not.
 - [12] C. Wu, B. A. Bernevig, and S.-C. Zhang, Phys. Rev. Lett. **96**, 106401 (2006).
 - [13] C. Xu and J. E. Moore, Phys. Rev. B **73**, 045322 (2006).
 - [14] See e.g. D. Sénéchal in *Theoretical Methods for Strongly Correlated Electrons*, eds. D. Sénéchal, A.-M. Tremblay, and C. Bourbonnais (Springer, Berlin, 2003).
 - [15] A. Furusaki and N. Nagaosa, Phys. Rev. B **47**, 4631 (1993).
 - [16] Q. P. Li, S. Das Sarma, and R. Joynt, Phys. Rev. B **45**, 13713 (1992).
 - [17] D. Goren, G. Asa, and Y. Nemerovskiy, J. Appl. Phys. **80**, 5085 (1996).
 - [18] C. L. Kane and M. P. A. Fisher, Phys. Rev. B **46**, 15233 (1992); Phys. Rev. B **51**, 13449 (1995).
 - [19] G. D. Mahan, *Many-Particle Physics, 3rd ed.* (Kluwer Academic/Plenum Publishers, New York, 2000).
 - [20] X.-G. Wen, Phys. Rev. B **44**, 5708 (1991).
 - [21] C.-Y. Hou, E.-A. Kim, and C. Chamon, Phys. Rev. Lett. **102**, 076602 (2009).